

Inhomogeneities of Stratocumulus Liquid Water

Robert F. Cahalan

Laboratory for Atmospheres, Goddard Space Flight Center

Jack B. Snider

NOAA/ERL/Wave Propagation Laboratory

There is a growing body of observational evidence on inhomogeneous cloud structure, most recently from the extensive measurements of the FIRE field program (Albrecht et al., 1988). Knowledge of cloud structure is important because it strongly influences the cloud radiative properties, one of the major factors in determining the global energy balance. Current atmospheric circulation models use plane-parallel radiation, so that the liquid water in each gridbox is assumed to be uniform, which gives an unrealistically large albedo, forcing the models to divide the liquid water by a "fudge factor" to get the albedo right (Harshvardhan and Randall, 1985). In reality cloud liquid water occupies only a subset of each gridbox, greatly reducing the mean albedo. If future climate models are to treat the hydrological cycle in a manner consistent with energy balance, a better treatment of cloud liquid water will be needed.

FIRE concentrated upon two cloud types of special interest: cirrus and marine stratocumulus. Cirrus tend to be high and optically thin, thus reducing the effective radiative temperature without increasing the albedo significantly, leading to an enhanced greenhouse heating. In contrast, marine stratocumulus are low and optically thick, thus producing a large increase in reflected radiation with a small change in emitted radiation, giving a net cooling which could potentially mitigate the expected greenhouse warming. The FIRE measurements in California stratocumulus during June and July of 1987 show variations in cloud liquid water on all scales. Boers and Betts (1988) describe the vertical structure, while Cahalan and Snider (1989, hereafter CS) discuss horizontal variations, which is our focus here. Such variations are associated with inhomogeneous entrainment, in which entrained dry air, rather than mixing uniformly with cloudy air, remains intact in blobs of all sizes, which decay only slowly by invasion of cloudy air. The following paragraphs describe two important stratocumulus observations, then follows a simple fractal model which reproduces these properties, and the paper concludes by briefly discussing the model radiative properties.

Vertically integrated liquid water was measured at 10 Hz and averaged over

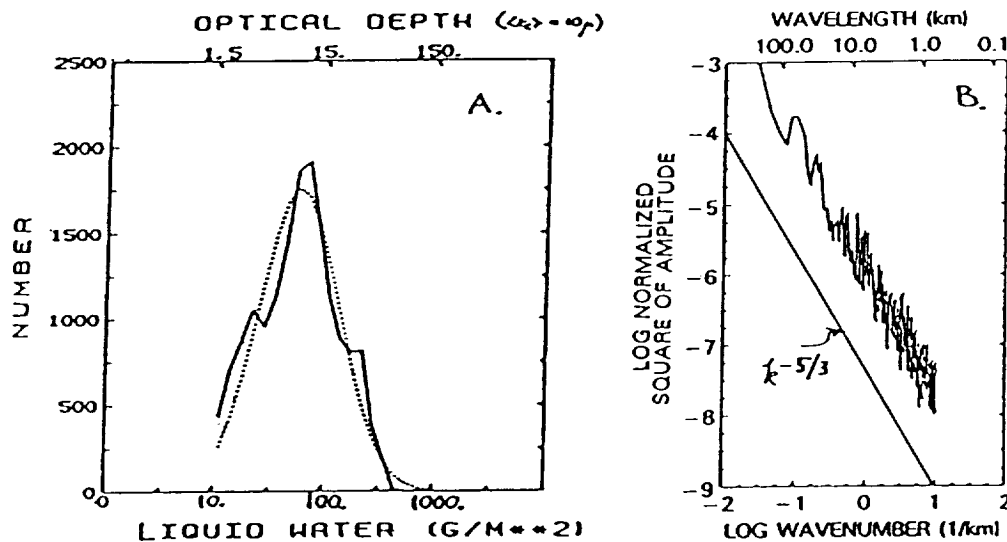


Figure 1: (a) Histogram of logarithm of vertically integrated stratocumulus liquid water in mm along with a lognormal fit. The equivalent optical depth scale shown at the top assumes a 10 micron effective radius. (b) Wavenumber spectrum of integrated liquid water computed from time series assuming 5 m/s frozen turbulence.

1 minute intervals during a 3-week period on San Nicolas Island. The histogram of this data is shown in the first figure on a log-linear scale, with a lognormal fit plotted for comparison. The lognormal roughly follows the data, while differing in detail. The “shoulders” seen to each side of the observed central peak are a reminder that individual days often show a bimodal distribution.

The liquid water wavenumber spectrum shown in the second figure was estimated from the frequency spectra computed from several 1-day time series from the same 19-day data set used for the histogram. Results were translated from frequency to wavenumber assuming frozen turbulence with a 5 m/s mean advection. The least-squares fit over the mesoscale regime from about 400 km down to about 400 m gives $S(k) \sim k^{-5/3}$.

This is the spectrum expected from a “passive” scalar (i.e. a scalar field whose variations in space and time are due only to advection.) when energy from a small-scale source (convection) is being transferred to larger scales by 2-dimensional homogeneous turbulence (Kraichnan, 1967; Lilly, 1989). This mesoscale 5/3 power spectrum was previously observed in velocity and potential temperature spectra from commercial aircraft data (Gage and Nastrom, 1986). The fact that the mesoscale liquid water spectrum is that expected for a 2-dimensional passive scalar — one being forced by small-scale convection — suggests that the total integrated liquid water in stratocumulus clouds fluctuates with the mesoscale-averaged vertical velocity, being large in updrafts and

small in downdrafts. This kind of behavior has been observed in fine-resolution numerical simulations (MacVean and Nicholls, 1988), though they do not reproduce the highly irregular fractal structure described above. At scales smaller than the cloud thickness (about 200 m) the spectrum drops off more rapidly, the slope being closer to -3 (CS). This within-cloud regime is still poorly understood, but is apparently not consistent with a 3-dimensional homogeneous cascade of energy from larger scales, which would also give a 5/3. The steep falloff could be related to the distribution of energy sources and sinks, including the active role of condensation, or to the inhomogeneity of the transfer process. More work is needed on the within-cloud regime, but the following focuses upon the mesoscale structure because of its greater impact on the large-scale energy balance.

In order to simulate the mesoscale fractal structure of stratocumulus liquid water, a procedure is needed to generate a random function having the probability and spectrum shown above. As a first step, variations in only one horizontal direction will be allowed, forming fractal streets, a simplified version of the cloud streets observed in the July 7 Landsat scene during FIRE (CS). Consider a stratocumulus cloud forming an infinitely long slab of horizontal width $L \approx 100\text{km}$ and a typical optical depth of, say, $\tau_0 = 10$. Divide this into two slabs of width $L/2$, and transfer a fraction f_1 of the liquid water from one half to the other, with the direction chosen at random. The optical depth in one half is then increased (by increasing the density — thickness is assumed unchanged), and the other half is correspondingly thinned. This may be written $\tau_1^{(\pm)} = (1 \pm f_1)\tau_0$, where the superscript on the left indicates whether the brighter or darker half is being considered.

To continue the process, each half is itself divided in half, and a fraction of liquid water, f_2 , is transferred, again in a random direction. After iterating for n cascade steps, there are 2^n segments, each with an optical depth of the form

$$\tau_n^{(\pm \dots \pm)} = \prod_{k=1}^n (1 \pm f_k) \tau_0, \quad (1)$$

where $0 < f_k < 1$. Any of the possible combinations of signs in (1) may be found somewhere among the 2^n segments. An upper bound on the optical depth of the optically thickest segment may be found from

$$\tau_{max} = \prod_{k=1}^n (1 + f_k) < \prod_{k=1}^n \exp(f_k) = \exp\left(\sum_{k=1}^n f_k\right). \quad (2)$$

Consider two cases: a “singular model” in which the fraction does not change with k (i.e. $f_k = f$), and a “bounded model” in which the fraction decreases (i.e. $f_k = fc^k$, where f and c are both constants between 0 and 1). The upper bound given by (2) diverges for the singular model, and one can show that the liquid water becomes concentrated on a fractal set of singularities as $n \rightarrow \infty$.

The upper bound for the bounded model is $\exp(fc/(1-c))\tau_0$, and is close to τ_{max} . It is possible to show that both models have a wavenumber spectrum of the form $S(k) \sim k^{-\alpha}$, where

$$\alpha = \begin{cases} 1 - \ln_2(1 + f^2), & \text{(singular model)} \\ 1 - \ln_2(c^2), & \text{(bounded model)} \end{cases} \quad (3)$$

Note that as $f \rightarrow 1$, the exponent of the singular model approaches zero, giving a flat spectrum, while as $f \rightarrow 0$ the spectrum steepens to k^{-1} . No value of f allows the singular model to fit the observed $k^{-5/3}$ spectrum. The exponent of the bounded model, on the other hand, gives $\alpha = 5/3$ if we choose $c = 2^{-1/3}$. The probability density is sensitive to c , and often shows considerable structure, but when $c = 2^{-1/3}$ it is close to lognormal, and similar to the first figure.

These simple models of one-dimensional fractal cloud streets can be generalized to allow variations in three dimensions and tuned to simulate other cloud types. The albedo and other radiation properties are computed by Monte Carlo techniques, and results are parameterized to provide alternatives to plane parallel theory. For the stratocumulus models the redistribution of liquid water at each iteration decreases the mean albedo from the plane parallel case, since the albedo of optically thick regions saturates for large optical depths, so that realistic amounts of cloud liquid water lead to realistic albedos (Cahalan, 1989). Much remains to be done both in documenting the global climatology of cloud fractal structure and in understanding the physical processes underlying this structure, but improved observations and more appropriate analytical tools are finally allowing the great complexity of cloud liquid water to be approximated as something other than a uniform distribution.

References

- Albrecht, B. A., D. A. Randall, and S. Nicholls (1988), Observations of marine stratocumulus clouds during FIRE, *Bull. Amer. Meteor. Soc.*, **69**, 618-626.
- Boers, R., and A. K. Betts (1988), Saturation point structure of marine stratocumulus clouds, *J. Atmos. Sci.*, **45**, 1156-1175.
- Cahalan, R. F. (1989), Overview of fractal clouds, in **Advances in Remote Sensing Retrieval Methods**, A. Deepak Publishing, pp. 371-389, xxiv + 519 pp.
- Cahalan, R. F., and J. H. Joseph (1989), Fractal statistics of cloud fields, *Mon. Wea. Rev.*, **117**, 261-272.
- Cahalan, R. F., and J. B. Snider (1989), Marine stratocumulus structure during FIRE, *Remote Sens. Environ.*, **28**, 95-107.

Gage, K. S. and G. D. Nastrom (1986), Theoretical interpretation of atmospheric wavenumber spectra of wind and temperature observed by commercial aircraft during GASP, *J. Atmos. Sci.*, **43**, 729-740.

Harshvardhan and D. A. Randall (1985), Comments on "The parameterization of radiation for numerical weather prediction and climate models", *Mon. Wea. Rev.*, **113**, 1832-1833.

Kraichnan, R. H. (1967), Inertial ranges in two-dimensional turbulence, *Phys. Fluids*, **10**, 1417-1423.

Lilly, D. K. (1989), Two-dimensional turbulence generated by energy sources at two scales, *J. Atmos. Sci.*, **46**, 2026-2030.

MacVean, M. K., and S. Nicholls (1988), A fine-resolution, two-dimensional numerical study of a cloud-capped boundary layer, Proceedings of the 10th International Cloud Physics Conference, Bad-Hamburg, FRG, August 15-20, pp. 425-427.

